Chapter 1. Global agroclimatic patterns

Chapter 1 describes the CropWatch agroclimatic indicators (CWAIs) for rainfall (RAIN), temperature (TEMP), and radiation (RADPAR), along with the agronomic indicator for potential biomass (BIOMSS) for sixty-five global Monitoring and Reporting Units (MRU). Rainfall, temperature, and radiation indicators are compared to their average value for the same period over the last fifteen years (called the "average"), while BIOMSS is compared to the indicator's average of the recent five years. Indicator values for all MRUs are included in Annex A table A.1. For more information about the MRUs and indicators, please see Annex C and online CropWatch resources at www.cropwatch.com.cn.

1.1 Overview

Rainfall

In many ways, the current reporting period from July to October 2016 displays some global patterns that were already noticed in the previous CropWatch bulletins, notably above-average rainfall in a large area including semi-arid sub-Saharan Africa and extending across the Arabian Peninsula to central Asia. This pattern has been ongoing for more than one year now. The largest excesses are those that occurred in the Asian part of the region, especially Southern Mongolia (MRU-47, RAIN +201%), Gansu-Xinjiang (MRU-32, +175%), and Inner Mongolia (MRU-35, +56%). As these areas already normally receive fair amounts in the July-October period, increases are significant. Smaller, but still marked excesses in the range from 25% to 30% occurred—from lower to higher increases—in Eastern Central Asia (MRU-52), the Chinese islands of Taiwan (MRU-42), Hainan (MRU-33), and the Lower Yangtze region (MRU-37) where precipitation reached 673 mm (168 mm/month on average and 33% above average). Further west, increases are also reported for western Asia (MRU-31, +28%), Punjab to Gujarat (MRU-48, +33%), and the Pamir Area (MRU-30, +35%) where the precipitation is welcome during the present pre-rabi crop season. Finally, at the western end of the area, increases also include a region from the Sahara to Afghan deserts (MRU-64, +41%) leading to Gulf of Guinea countries (MRU-03, +11%) and across the Sahel (MRU-08) where the excess of 15%, while modest, has nevertheless benefited the end of the semi-arid crop areas in western and northern-central Africa.

Other notable rainfall excesses included Maritime South-east Asia (MRU-49), which recorded an increase of precipitation over average reaching 25%, while northern Australia (MRU-53) recorded a large positive departure that more than doubled the average (+127%).

In North America, the pattern of large excesses in the northernmost areas (which are of limited relevance for crops) also continued this year. The excess also affected British Columbia to Colorado (MRU-11, +40%), the West Coast (MRU-16, +45%), and particularly the northern Great Plains (MRU-12, with rainfall nearly double the average: +97%).

In South America, the Brazilian Nordeste (MRU-22) is the only area that recorded a precipitation excess (+26%).

Precipitation deficits reproduced recent patterns in east and southern Africa, including in the East African Highlands (MRU-02, -24%); the Horn of Africa (MRU-04, -40%) and Southwest Madagascar (MRU-06, also -40%); and Southern Africa (MRU-09, -11%) and Western Cape (MRU-10, -58%). Water reserves are low

from the previous season's drought throughout the region, but the current agricultural season is just starting in the south.

In South America, dry conditions affect some areas where cattle plays a larger role than crops, such as Western Patagonia (MRU-27, -36%).

The previous CropWatch bulletin stressed the Korean and the Moroccan drought. North Africa-Mediterranean (MRU-07) is currently suffering a RAIN deficit (-14%) that extends into Western Europe (MRU-60, also -14%) but intensifies in the east of the region in Mediterranean Europe and Turkey (MRU-59, -26%) and the Caucasus (MRU-29, also at -26%). The eastern Asian areas (MRU-43, i.e. the Republic of Korea, Democratic People's Republic of Korea, and the Primorsky area of Russia and Northern Japan) and MRU-46 (Southern Japan) experienced deficits of 28% and 14%, respectively.

In both New Zealand (MRU-56) and Nullarbor to Darling (MRU-55) the RAIN deficit reached between 50% and 60%.

Temperature

Low temperature anomalies were generally rare this reporting period and they usually concerned only isolated MRUs. The largest area, in terms of the number of adjacent MRUs affected, occured in Australia where the center and south of the continent (MRU-55, Nullarbor to Darling, to MRU-54, Queensland to Victoria) experienced cool spring condition with CropWatch TEMP anomalies ranging from -0.5°C in the east to -1.5°C in the west. In east and southern Africa, low temperature affected the Horn of Africa (MRU-04, TEMP -0.7°C) and the two Malagasy MRUs (MRU-5, -0.7°C and MRU-6, -1.0°C). Next are two adjacent areas in South America: Central-north Argentina (MRU-25, -1.2°C) and the Pampas (MRU-26, -0.7°C). Also worth mentioning is the Caucasus (MRU-29) with -0.7°C, before finally listing some positive anomalies in southern Japan and the southern tip of the Korean peninsula (MRU-46, +1.9°C) as well as northern Australia (MRU-53) with a +1.5°C departure.

Radiation

With RADPAR, some well-marked spatial patterns exist again, with excess radiation in the tropical and equatorial parts of the American continent and Africa: +3.1% in the Amazon (MRU-24), +4.3% in northern South and Central America (MRU-19), as well as +4.8% in the central-northern Andes (MRU-21), a significant value for a sunshine departure over a large area. The largest departure occurred in equatorial central Africa (MRU-01, +7%) covering essentially the Congo basin, with the adjacent Horn of Africa (MRU-4) recording a 4.2% positive RADPAR departure.

Negative RADPAR departures in agriculturally important locations concern basically all of Oceania, maritime Southeast Asia, and the whole Asian continent east of the latitude of MRU-48 (Punjab to Gujarat), with the exception of Qinghai-Tibet (MRU-39). This includes, among others, the following, in decreasing order of deficit: the lower Yangtze in China (MRU-37, RADPAR -7.9%), New Zealand (MRU-56, -74%), Queensland to Victoria (MRU-54, -7.3%), northern Australia (MRU-53, -5.4%), Taiwan (MRU-42, -5.0%), and Punjab to Gujarat (-4.9% in MRU-48).

Combinations of anomalies

For the reporting period, generally, little coherence existed between RAIN and other environmental variables, except BIOMSS, which is directly influenced by water availability. At the scale of MRUs, a reasonably good negative correlation between large excesses of rainfall and sunshine (RADPAR) is visible, mostly in Southern Mongolia (MRU-47, RAIN +201% and RADPAR -2.9%), Gansu-Xinjiang (MRU-32, +175%, -3.4%), Northern Australia (MRU-53, +127%, -5.4%) and the northern Great Plains in the United States

(MRU-12, +97% and -4.6%). (This correlation is more marked at finer spatial resolution, see section 3.1). In the four areas, BIOMSS departure were respectively: +97%, +132%, +89%, and +58%.

While quite some MRUs experienced a "double anomaly"—for example excess RAIN and RADPAR—only few "triple anomalies" are seen. One, however, is in MRU-04, the Horn of Africa, which suffered from drought (RAIN, -41%) combined with low temperature (-0.7°C), and, paradoxically, abundant RADPAR (+4.3%). Another, northern Australia (MRU-53), on the contrary recorded abundant rainfall (+127%), high temperature (+1.5°C), and a shortage of sunshine (RADPAR -5.4%).

Figure 1.1. Global map of July-October 2016 rainfall anomaly (as indicated by the RAIN indicator) by MRU, departure from 15YA (percentage)

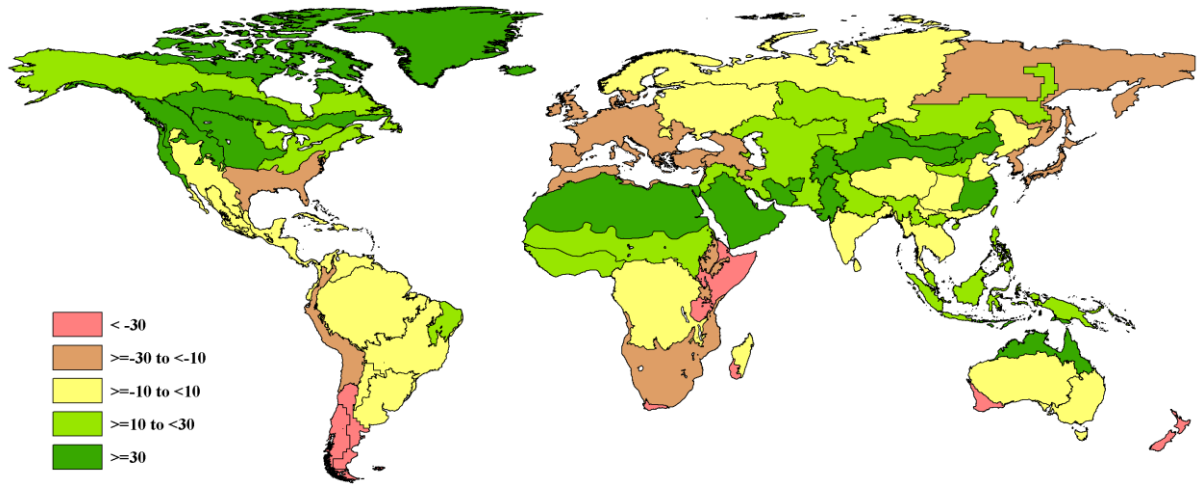

Figure 1.2. Global map of July-October 2016 temperature anomaly (as indicated by the TEMP indicator) by MRU, departure from 15YA (degrees Celsius)

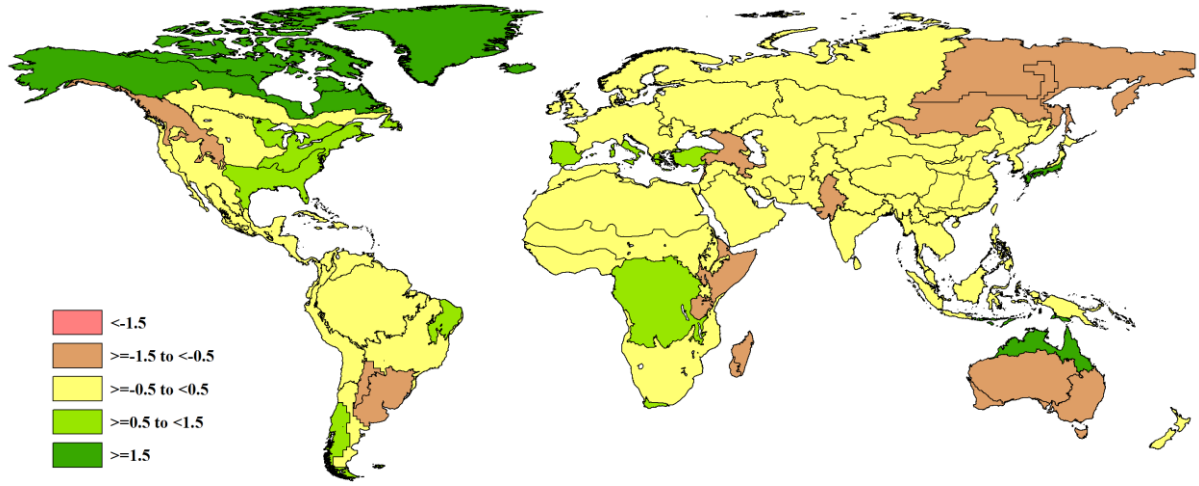

Figure 1.3. Global map of July-October 2016 PAR anomaly (as indicated by the RADPAR indicator) by MRU, departure from 15YA (percentage)

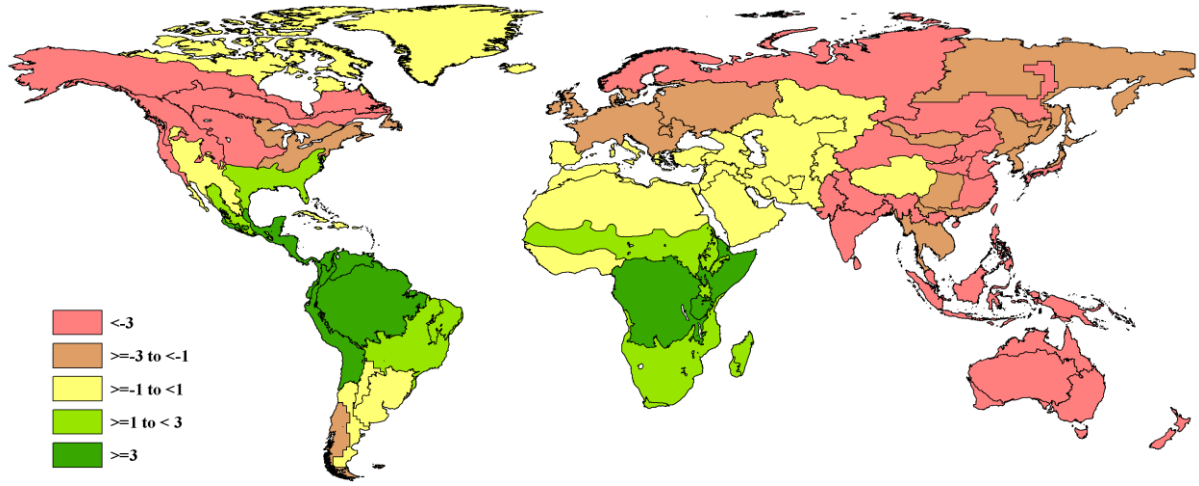

Figure 1.4. Global map of July-October 2016 biomass accumulation (BIOMSS) by MRU, departure from 5YA (percentage)